Jurnal Teknologi, 36(D) Jun 2002: 129–143

MODELLING TECHNIQUES FOR RECTANGULAR DIELECTRIC WAVEGUIDES – RIBS WAVEGUIDES

ABU SAHMAH MOHD SUPA'AT[1], ABU BAKAR MOHAMMAD[2] & NORAZAN MOHD KASSIM[3]

Abstract. Rectangular dielectric waveguides have been known as a basic device structure in integrated optics. Result of waveguide analysis is very useful in the study of mode propagation characteristics in a waveguide. In this paper optical propagation in dielectric waveguides have been analyzed using the semi analytical effective index method and a numerical method based on finite difference approach. Full waveguide cross-section and open boundary condition have been considered. This models the exponential decay field at a sufficient distance. Both the propagation characteristic and the field of the guided modes can be calculated very efficiently on a personal computer with modest computational time. This method is applied to the well established test structured for a ribs waveguides. Comparison has been made and some limitations to accuracy have been identified.

Keywords: Dielectric waveguide, Propagation characteristic, Effective index method, Finite difference, Open boundary condition

1.0 INTRODUCTION

The use of optical signals as a means of carrier in telecommunications is evident since the invention of laser in 1960 [1]. It was in 1969, Miller introduced the term 'Integrated Optics' involves the realization of optical and electrooptic elements which may be integrated in the large numbers on one chip by means of the same processing techniques used to fabricate integrated electronic circuits [2]. Demand for integrated optic circuits comes from the side of lightwave communication systems which require in addition to laser source, components such as optical switches, modulators and power splitters.

Recent advances in material growth and processing technologies mean that the refractive index, geometric profile and the theoretical analysis of their propagation properties are receiving much interest. In this paper we considered passive waveguide discussed in Section 2.0 and rib waveguide, which are the simplest integrated optical components. In all cases the guided light is confined in a region of increased refractive index or effective index. To determine the accuracy of our modeling techniques, the results obtained have been compared with other techniques and different methods presented in [3][9].

[1,2&3] Photonic Research Group, Faculty of Electrical Engineering, Universiti Teknologi Malaysia, 81310 UTM Skudai, Johor Darul Takzim. e-mail: abus@fke.utm.my

2.0 DIELECTRIC WAVEGUIDES

Dielectric waveguides are the structures that confine and guide the light in the guided-wave devices and circuits of integrated optic in a region of higher effective index than its surrounding media. A well known dielectric waveguide is optical fiber which usually has a circular cross-section. In contrast, the guides of interest to integrated optics are usually planar structures such as planar film or strip. Figure 1 illustrates the cross-section of four strip waveguide types that have been investigated in integrated optics. Figure 1(a)-(d) depict four different structures of strip waveguides, in which the optical energy is confined in the region which has the highest index of refraction, thus providing the guiding region. In all four examples, the light is more or less confined to the material with index $n_f > n_s, n_c, n_1$. The superstrate, n_c is normally air with index of refraction of 1.0. For symmetric waveguide, both the substrate and the superstrate have the same refractive index, otherwise it becomes asymmetric or composite structures [4].

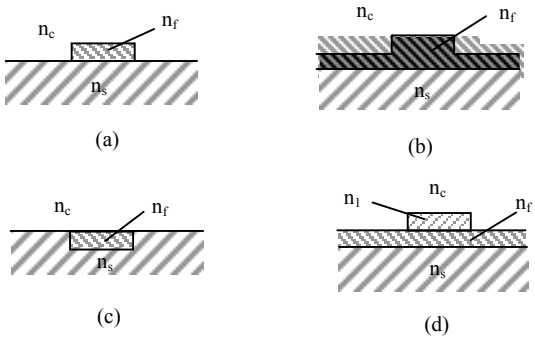

Figure 1 Various strip waveguide structures (a) raised strip (b) ridge guide (c) embedded strip and (d) strip-loaded guide

Depending on the index difference, the thickness for single mode operation varies, a typical thickness of the order of the optical wavelength. The index of refraction of the thin film of dielectric waveguide can be either homogeneous or graded in which index profile is primarily result of the waveguide fabrication process.

A raised strip guide can be fabricated by starting with a planar slab guide, masking the strip and removing the surrounding film by sputtering or etching techniques. Masked diffusion or ion implantation leads to embedded strip guides. The ridge guide can be made by techniques similar to the raised strip guide but with incomplete removal of the surrounding film and the final example shows a strip loaded guide where a strip of lower index $n_1 < n_f$ is deposited onto a planar guide.

2.1 Plane Wave Analysis of Dielectric Waveguide

Although the early analysis of propagating modes in the slab was based on the ray optic approach, here a wave optic approach is considered since it gives a complete description as that provided by electromagnetic theory. For simplicity we assume that the cladding regions with indices n_c and n_s are semi infinite in extent and that the film is of thickness 2d. The dielectric slab waveguide is also considered to be formed from materials which are linear, isotropic and source free.

To understand the co-ordinate system used, reference can be made to Figure 2 for a 3-layer slab waveguide where the x-axis represents the transverse direction and z-axis, represents the direction of propagation. However, to determine the full mode set and mathematical expressions for the fields it is best to seek solutions of Maxwell's equations and the wave equation directly. One set of solution has E in the y direction and these are the Transverse Electric (TE) modes. The other set with H in the y direction are Transverse Magnetic (TM) modes. The wave equation for the electric and magnetic field may be derived from Maxwell's equation and can be written as [5].

$$\nabla^2 \bar{E} = \mu\varepsilon \frac{\partial^2 \bar{E}}{\partial t^2} \quad \text{for TE mode} \tag{1}$$

$$\text{and } \nabla^2 \bar{H} = \mu\varepsilon \frac{\partial^2 \bar{H}}{\partial t^2} \quad \text{for TM mode} \tag{2}$$

where $\mu = \mu_0\mu_r$ and $\varepsilon = \varepsilon_0\varepsilon_r$.
μ_0 and ε_0 are the permeability and permittivity of free space respectively.
μ_r and ε_r are the relative permeability and permittivity of the materials respectively.

To simplify things further we again restrict to TE modes in which the only non-zero component of the electric field is *Ey* in the coordinate system used above. The wave equation then becomes [5],

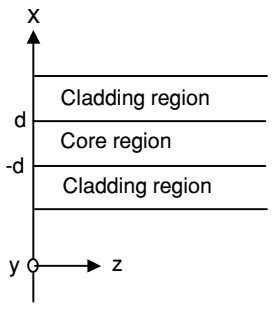

Figure 2 Schematic diagram of three layers slab waveguide structure

$$\frac{\partial^2 \bar{E}y}{\partial x^2} + \frac{\partial^2 \bar{E}y}{\partial z^2} = \mu\varepsilon \frac{\partial^2 \bar{E}y}{\partial t^2} \tag{3}$$

Since we are seeking guided wave propagating in the z direction, let,

$$\bar{E}y = \bar{E}_0(x)e^{j(wt-k_z z)} \tag{4}$$

where E_0 is the amplitude of the wave which varies across the guide. Substituting into equation (3) gives,

$$\frac{\partial^2 \bar{E}_0}{\partial x^2} - k_z^2 \bar{E}_0 = -w^2 \mu\varepsilon \bar{E}_0 \tag{5}$$

The factor $w^2\mu\varepsilon$ is equal to k^2, the magnitude of the wavevector in the dielectric, therefore equation (5) can be rewritten as,

$$\frac{\partial^2 \bar{E}_0}{\partial x^2} + (k^2 - k_z^2)\bar{E}_0 = 0 \tag{6}$$

From the vector triangle for the wavevector, $(k^2 - k_z^2) = k_T^2$ where k_T is the transverse component of $\hat{\mathrm{k}}$. Thus we have, substituting into equation (6),

$$\frac{\partial^2 \bar{E}_0}{\partial x^2} + k_T^2 \bar{E}_0 = 0 \tag{7}$$

From equation (7), we know something about the form of a guided mode and assuming k_T to be real in the core and imaginary in the cladding. To be consistent with the notation employed above let $k_T = k_{1x}$ in the core and $k_T = -j\gamma$ in the cladding. Using these the wave equation becomes,

$$\frac{\partial^2 \bar{E}_0}{\partial x^2} + k_{1x} \bar{E}_0 = 0 \quad \text{in the core} \tag{8}$$

and

$$\frac{\partial^2 \bar{E}_0}{\partial x^2} - \gamma^2 \bar{E}_0 = 0 \quad \text{in the cladding} \tag{9}$$

Solving (8) and (9) give,

$$E_0 = A\cos(k_{1x}x) + B\sin(k_{1x}x) \text{ in the core} \tag{10}$$

and

$$E_0 = Ce^{\gamma x} + De^{-\gamma x} \text{ in the cladding} \tag{11}$$

From (10) the solution in the core consists of a symmetric and asymmetric parts which correspond to the even and odd modes. For symmetric modes we can set B=0 and the expression for the electric field in the core becomes,

$$Ey = A\cos(k_{1x}x) \tag{12}$$

and in the cladding we can reject solutions which grow exponentially away from the core, thus,

$$E_0 = Ce^{\gamma x} \quad \text{for } x < -d \quad \text{and} \tag{13}$$

$$E_0 = De^{-\gamma x} \quad \text{for } x > d \tag{14}$$

From the electromagnetic boundary conditions, the tangential component of the electric field is continuous across the boundary and furthermore, in this case no current flows in the interface, the tangential of the magnetic field is also continuous. Dealing first with the electric field component, we have,

$$A\cos(k_{1x}x) = Ce^{\gamma d} \quad \text{continuity at } x = -d \tag{15}$$

$$A\cos(k_{1x}x) = De^{-\gamma d} \quad \text{continuity at } x = d \tag{16}$$

Dividing these yields the intuitively obvious result that $C = D$ and for the asymmetric modes the result would be $C = -D$.

In the TE modes we are considering, the magnetic field has only x and z components and of these only the z component is tangential to the interface and must therefore be continuous. From Maxwell's equation for $\nabla \times \bar{E}$, we can show that $\bar{H}z$ in this case is proportional to $\frac{\partial \bar{E}y}{\partial x}$. Hence differentiating the expressions for $\bar{E}y$ and equating at $x = d$ and $x = -d$, give,

$$-k_{1x}A\sin(k_{1x}d) = -\gamma Ce^{-\gamma d} \tag{17}$$

Dividing equation (17) by equation (15) and rearranging then yields,

$$\tan\left(k_{1x}d - \frac{n\pi}{2}\right) = \frac{\gamma}{k_{1x}} \tag{18}$$

for symmetric and asymmetric modes, where n is the mode number.

All the eigenvalues derived can be solved either a numerical or graphical methods. Once k_T is solved from equation (7), the propagation constant k_z or β can be obtained and the field distribution can be computed. Example of the transverse electric field

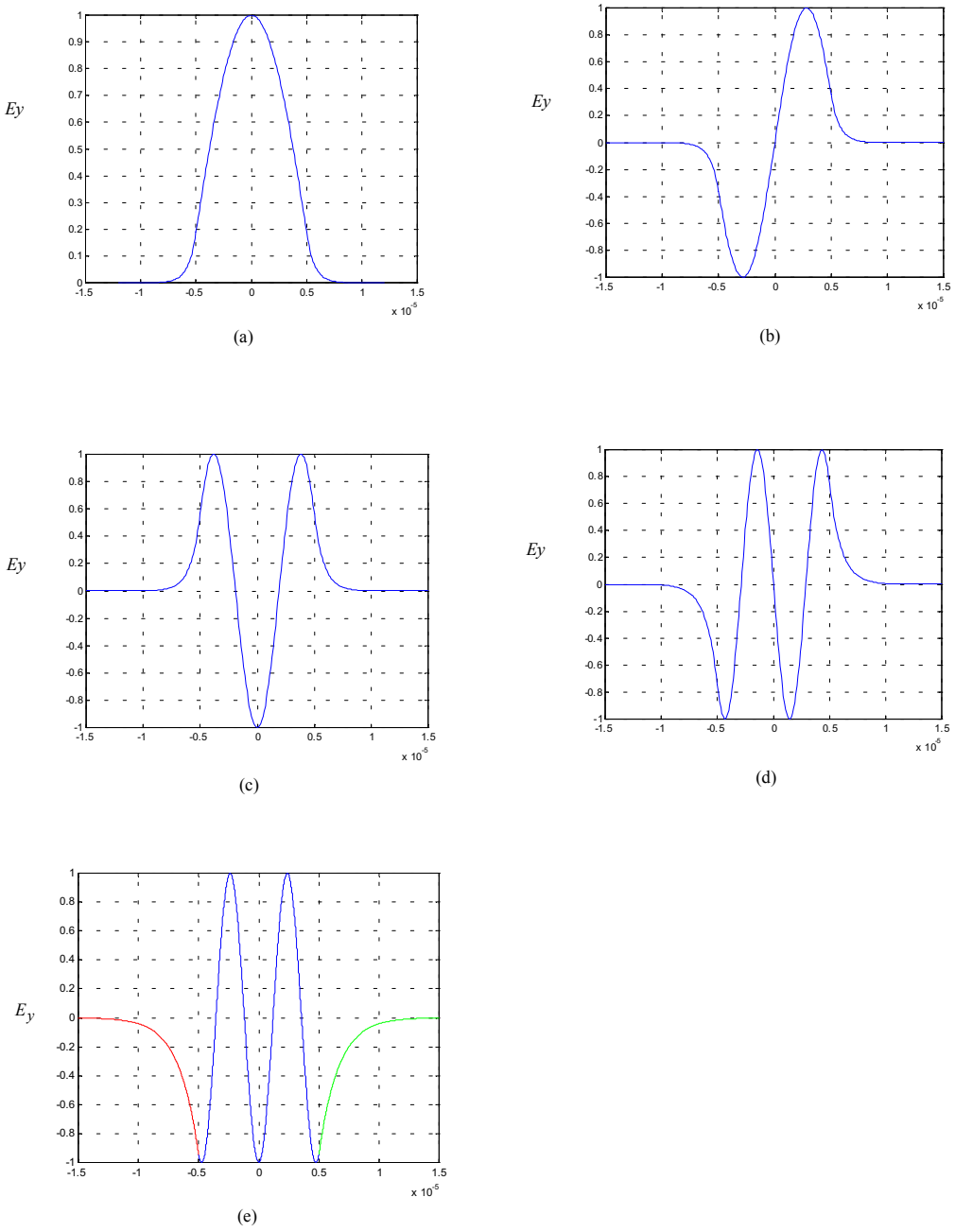

Figure 3 E field profiles for four symmetric and asymmetric TE modes for a given structure of d = 5 μm, λ = 1.55 μm, n_{core} = 1.61 and n_{sub} = 1.569. (a) TE_0 (b) TE_1 (c) TE_2 (d) TE_3 and (e) TE_4. Ey has been normalized to 1 and y axis is in m

profiles computed and plotted is as shown in Figure 3. All together five TE modes exist in this example with a guiding layer thickness 2d, of 10 μm, wavelength used 1.55 μm, the refractive indices of guiding layer, $n_{core} = 1.61$, substrate layer, $n_{sub} = 1.569$ and the cladding layer is taken as the same as substrate layer respectively.

2.2 Analysis By Effective Index Method

The planar dielectric waveguide mentioned above in Figure 2 provide no confinement of light within the film plane, that is the y-z plane, and confinement take place in the x-dimension only. Dielectric strip waveguides mentioned in Figure 1, which also called 3-dimensional guide provide this additional confinement, which we assume to be in y-dimension. The values of the indices and the dimensions of guide define the modes propagation and their corresponding field pattern. The formation of channels which are dimensionally precise and structurally smooth is essential for low-loss waveguide devices. An approximate solution to this particular structure for cases sufficiently far away from cut-off is shown in [6]. Another simple tool providing fairly good predictions for the behavior of channel guides is the effective index method [7]. One of the advantage of this method is that the problem can be reduced to solving the eigenvalue for the slab waveguide to obtain the effective refractive index of each region. To illustrate the method here, we choose the example of rectangular waveguide as shown in Figure 4.

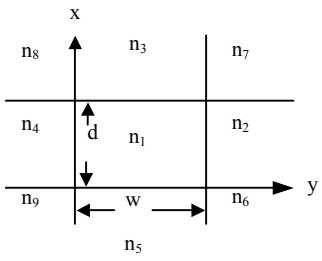

(a) A rectangular dielectric waveguide

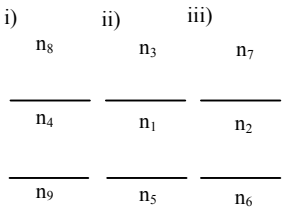

(b) Step one: Solve for each y the effective index $n_{eff}(y)$

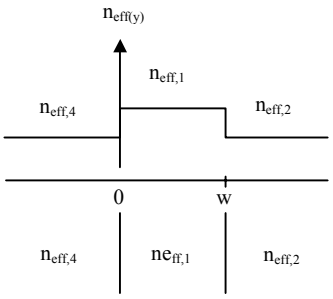

(c) Step two: Solve the slab waveguide problem using $n_{eff}(y)$

Figure 4 (a) A rectangular dielectric waveguide to be solved using the effective index method. (b) Solve the slab waveguide problem for each y and obtain effective index profile $n_{eff}(y)$. (c) Solve the slab waveguide problem with the effective index problem $n_{eff}(y)$

We first solved a slab waveguide problem with refractive index n_1 inside and n_3, n_5 outside the waveguide in Figure 4(b). The eigenequation for the *Ey* component will be that discussed in the preceeding sections. From the solutions of the slab waveguide problem, we obtained the propagation constant and hence the effective index $n_{eff,1}$. For $y > w$ or $y < 0$ similar equations hold for $n_2 > n_6$, n_7 and $n_4 > n_8$, n_9. Otherwise, approximations have to be made by assuming that $n_{eff,2} = n_2$ and $n_{eff,4} = n_4$ when the fields in regions 6, 7, 8, 9 are negligible. We then solved the slab waveguide problem as shown in Figure 4(c).

2.3 Analysis By Numerical Approach

The finite difference solution of the scalar wave equation has been applied to the rib waveguide problem for several years [8][9][10]. The basis of the procedure is to replace the wave equation by finite difference relations in terms of the field at discrete mesh points. In our analysis the mode is assumed to be TE mode propagating in the z direction and of the scalar form given by,

$$E_x(x,y,z) = E_x(x,y)e^{j(wt-\beta z)} \tag{19}$$

where β is the propagation constant and $E_x(x,y)$ is the optical field distribution. $\beta = \dfrac{2\pi n_{\text{eff}}}{\lambda}$ where n_{eff} is the modal effective index. The wave equation is given by [5],

$$\frac{\partial^2 \overline{E}}{\partial x^2} + \frac{\partial^2 \overline{E}}{\partial y^2} + k_T^2 E = 0 \tag{20}$$

The parameter k_T determines the propagation constant β through,

$$k_T^2 = w^2\mu\varepsilon - \beta^2 \tag{21}$$

The eigenvalue problem is to solve for $E(x,y)$ and k_T simultaneously so that equation (20) is satisfied. Since our problem involve very large matrices, the iterative solution is clearly needed to get better results. A variational method is used to established the propagation constant of the mode after each iteration and convergence of this value is the criterion for sufficient accuracy. The variational expression is derived from the wave equation (20) for TE modes and is given by,

$$\beta^2 = \frac{\iint (\nabla_t^2 E + k^2 n^2(x,y)E)E^* dxdy}{\iint E \cdot E^* dxdy} \tag{22}$$

In our analysis full waveguide cross section with open boundary condition has been considered. This models the field at the boundary of the waveguide will exponentially decay at a sufficient distance. To use the finite difference method a mesh point is

established throughout the waveguide cross section with a rectangular mesh of size h_x and h_y in the x and y direction respectively. Using Taylor's theorem and after some rearrangement to equation (22) becomes,

$$\beta^2 = \frac{\sum_i \sum_j E(i,j)\left[E(i+1,j)+E(i-1,j)+E(i,j+1)+E(i,j-1)+k^2 n^2(i,j)E(i,j)\right]}{\sum_i \sum_j \left[E(i,j)\right]^2} \tag{23}$$

and the iterative process after the determination of optimum acceleration factor for successive over relaxation (SOR) method is given by,

$$E^n(i,j) = E^{n-1}(i,j) + R\left[\frac{P\left[E^{n-1}(i+1,j)+E^{n-1}(i-1,j)\right]+E^{n-1}(i,j+1)+E^{n-1}(i,j-1)}{2(P+1)-k_T h_y^2} - E^{n-1}(i,j)\right] \tag{24}$$

where $P = \frac{h_y}{h_x}$ and R is the acceleration factor as an improvement that speed the convergence process derived from the successive over relaxation method which increases the rate of convergence by a factor of three. Values of R greater than unity speed convergence but to large a value of R results in numerical instability [11][12]. In our analysis its value is taken to be 1.4. The integrands in this analysis are evaluated numerically using trapezoidal rule. Alternate use of equations (23) and (24) should converge to a solution for E and β and which mode is converge to depends on the initial conditions.

3.0 RESULTS AND DISCUSSION

In order to determine the accuracy of our modelling techniques for calculating the eigenmodes of integrated optical waveguides we compared our results with other techniques presented in [3][9]. The rib waveguide structure studied is shown in Figure 5. The waveguide operates at a wavelength, λ = 1.55 μm. Its width is 2.4 μm and the thickness d of the guiding layer is 0.2 μm. The thickness t has been varied from 0 to 0.4 μm. The numerical results given in Figure 6 are the normalized propagation constant b of the fundamental TE mode. The height h of the ridge is chosen to be large enough so that it will not influence the results. The normalized propagation constant b is defined as,

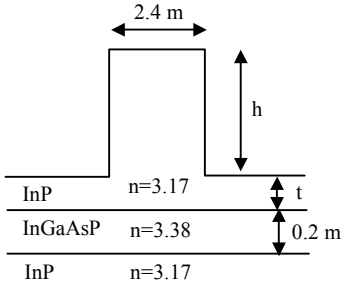

Figure 5 Schematic diagram of the III-V integrated optical waveguide operating at 1.55 μm

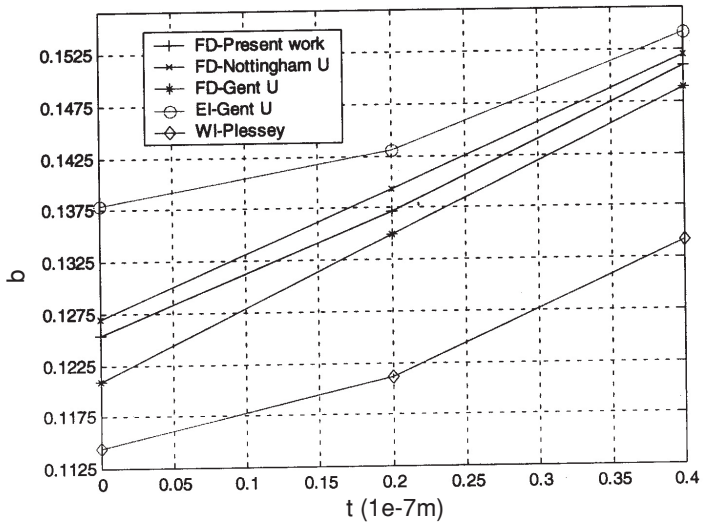

Figure 6 Normalized effective indices as a function of t for the structure shown in Figure 5

$$b = \left(\frac{n_{\text{eff}}^2 - n_{\text{sub}}^2}{n_{\text{guide}}^2 - n_{\text{sub}}^2} \right) \pi \tag{25}$$

with $n_{\text{sub}} = 3.17$ and $n_{\text{guide}} = 3.38$. The effective index, n_{eff} of the fundamental mode is related to the propagation constant β by,

$$n_{\text{eff}} = \frac{\beta\lambda}{2\pi} \tag{26}$$

From the graph shown in Figure 6 it can be seen that the results of effective index (EI) and weighted index (WI) methods give an upper bound and lower bound normalized effective index, b respectively. Result obtained by our modelling technique does appear within these limits and agree well with other techniques. However there are still some difference and some of these may be due to the meshing effects and rounding of errors. The second well established test structures is as shown in Figure 7. The

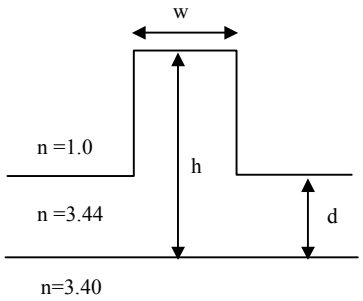

Figure 7 Schematic diagram of the GaAs waveguide structure operating at 1.15 μm

waveguide operates at a wavelength, λ = 1.15 μm. The width, w = 3 μm and the height of the ridge, h = 1 μm and the thickness d has been varied from 0.1 μm to 0.9 μm.

The graphs have been plotted for the modal index, n_{eff} and the normalized efffective index, b as shown in Figure 8 and 9 respectively. Our models, FD and EI methods agree well to those produced by the vector finite element (VFE), semi vectorial finite difference (SVFD) and full vectorial finite difference (FVFD) methods. Three dimensional and contour plots of light intensity distribution calculated from FD method on structures shown in Figure 5 and 7 for TE modes are also shown in Figure 10(a) and (b) and 11(a) and (b) respectively.

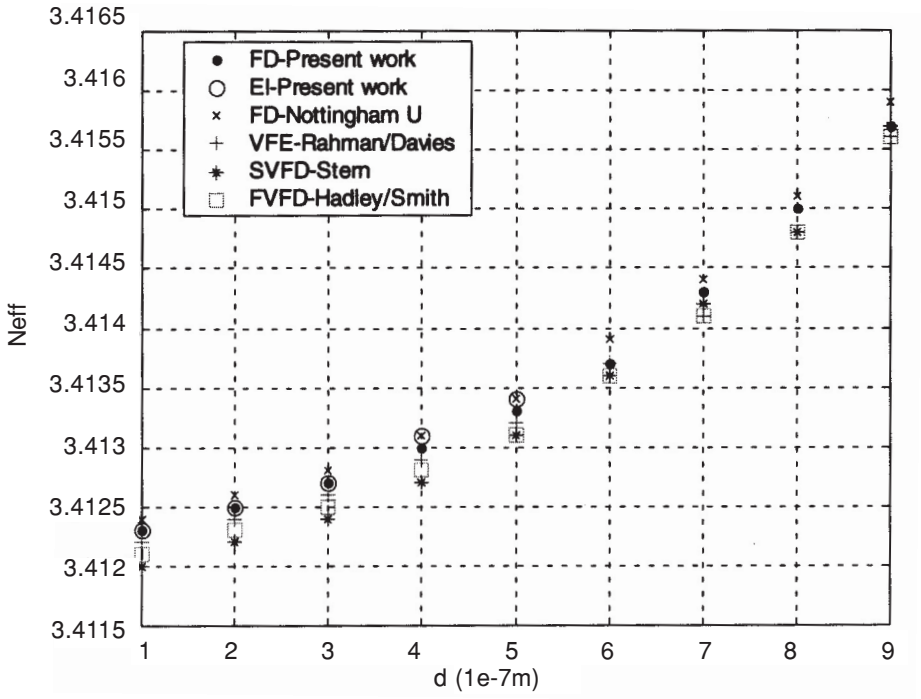

Figure 8 Mode effective indices as a function of d for the structure shown in Figure 7

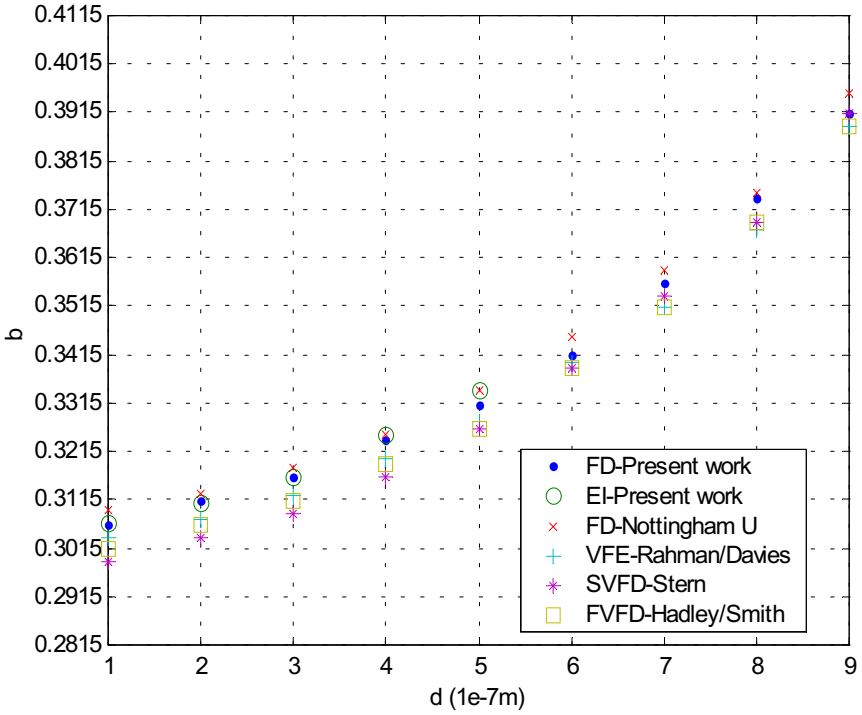

Figure 9 Normalized effective indices as a function of d for the structure shown in Figure 7

4.0 CONCLUSIONS

The EI method and the itterative solution implementation of scalar FD have been shown to be agreeable with most of the standard well known techniques discussed above. For the ridge waveguide it is shown that the EI method give very good result with the FD up to d = 0.4 μm. EI method is usually accurate particularly when the waveguide has an aspect ratio far from unity. Near the cut-off the EI method will tend to give a slight overestimate for the value of the propagation constant. The mesh size will determine the accuracy of the field and propagation constant because the larger the mesh size, the less valid is the approximation of the FD equation to the wave equation. On the other hand, if the mesh size is too small the computational time is uneconomical. Therefore a compromise between them and suitable mesh size was then chosen.

ACKNOWLEDGEMENTS

The authors would like to thank the Ministry of Science, Technology and Environment (MOSTE) for financing this project under the National Top-Down photonics project. Our gratitude also goes to the administration of Universiti Teknologi Malay-

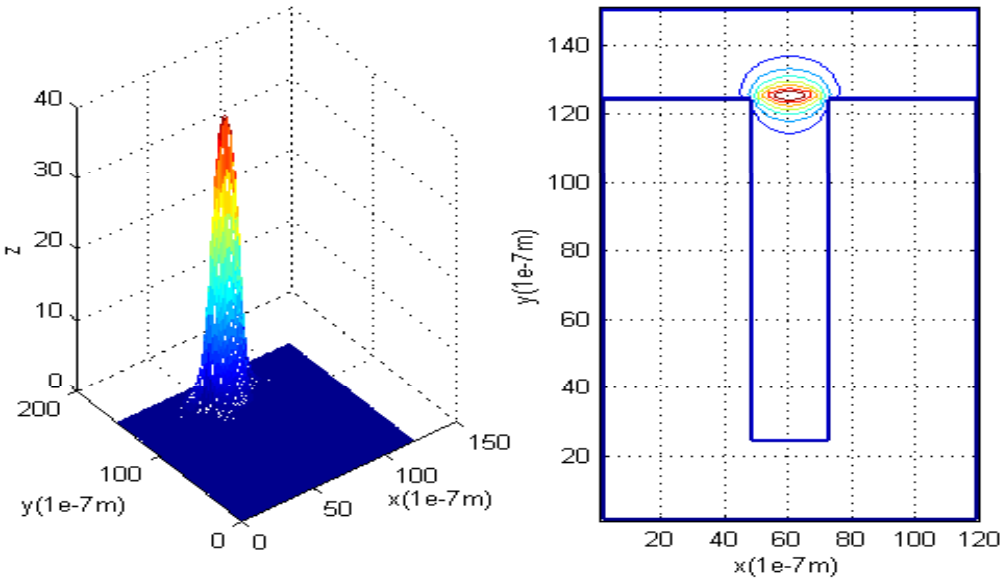

(a) t=0

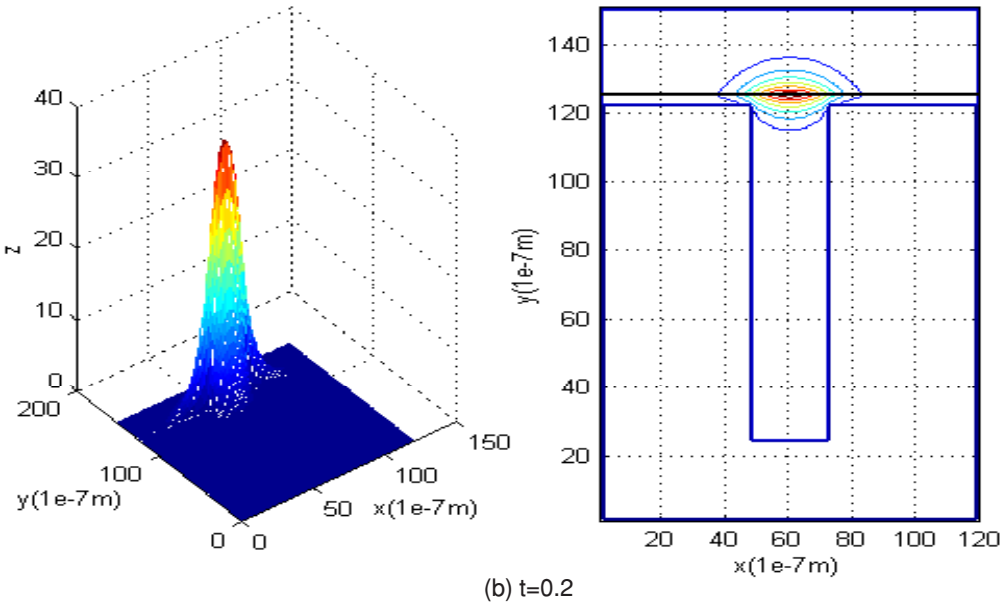

(b) t=0.2

Figure 10(a) and (b) Three dimensional and contour plot of light intensity distribution within the structure shown in Figure 5 for waveguide thickness t=0.0 and 0.2 respectively

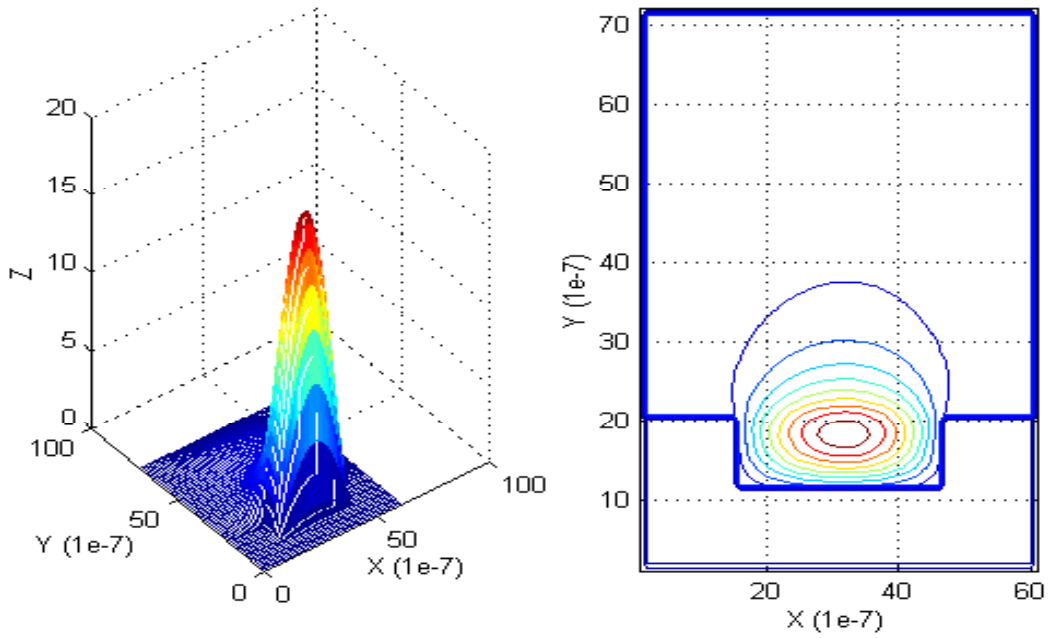

(a) d=0.1

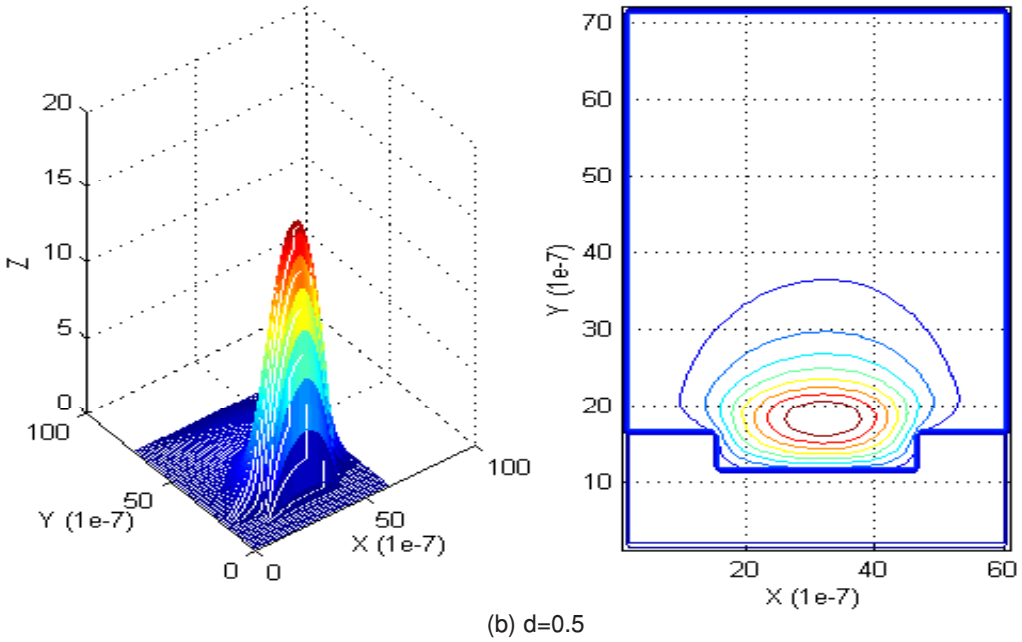

(b) d=0.5

Figure 11(a) and (b) Examples of three dimensional and contour plot of light intensity distribution within the structure shown in Figure 7 for d=0.1 and 0.5 μm respectively

sia (UTM) especially the Research Management Center (RMC) for their support and all members of Photonics Research Group UTM (PRG) for their invaluable help.

REFERENCES

[1] Palais, J. C. 1992. *Fiber optic communications*. Prentice Hall, Inc. A Simon & Schuster, Englewood Cliffs, New Jersey.
[2] Miller, S. E. 1969. *Integrated optic:An introduction*. Bell System Tech. J., 48(7): 2059 – 2069.
[3] Lagasse P. et al. 1988. *COST-216 comparative study of eigenmode analysis methods for single and coupled integrated optical waveguide*. 14th. European Conference on Optical Communications, IEE Conf. Publ. No. 292, Part 1, 296 – 299.
[4] Kogelnik, H. 1975. *Theory of dielectric waveguides –Topics in Applied Physics-Integrated Optics-edited by T. Tamir*. Vol. 7, Springer-Verlag, Berlin Heidelberg-New York, 15 – 79.
[5] Mohd Kassim, N. 1991. *Optical Waveguides in Silicon Materials*. PhD Thesis, University of Nottingham.
[6] Hunsperger, R. G. 1995. *Integrated Optics-Theory and Technology*. Springer-Verlag, Berlin Heidelberg-New York.
[7] Marom, E., O. G. Ramer, and S. Ruschin. 1984. *Relation between normal mode and coupled-mode analyses of parallel waveguides*. IEEE J. Quantum Electronics. 20(12): 1311 – 1319.
[8] Robertson, M. J., S. Ritchie, and P. Dayan. 1985. *Semiconductor waveguides: Analysis of optical propagation in single rib structures and directional coupler*. IEE Proceedings, 132(6): 336 – 342.
[9] Hadley, G. R., and R. E. Smith. 1995. *Full-vector waveguide modeling using an iterative finite-difference method with transparent boundary conditions*. Journal of Lightwave Tech., 13(3): 465 – 469.
[10] Lusse, P., P. Stuwe, J. Schule, and H. G. Unger. 1994. *Analysis of vectorial mode fields in optical waveguides by a new finite difference method*. J. of Lightwave Tech. 12(3): 487 – 493.
[11] William, F. A. 1992. *Numerical methods for partial differential equations*. Third edition, Academic Press, Inc.
[12] Booton, R. C. Jr. 1992. *Computational methods for electromagnetic and microwaves*. John Wiley & Sons, Inc.